Use and Misuse of Laplace's Law in Ophthalmology

Cheuk Wang Chung,[1] Michaël J. A. Girard,[1,2] Ning-Jiun Jan,[3,4] and Ian A. Sigal[3,4]

[1]Department of Biomedical Engineering, National University of Singapore, Singapore
[2]Singapore Eye Research Institute, Singapore National Eye Centre, Singapore
[3]Department of Ophthalmology, University of Pittsburgh School of Medicine, Pittsburgh, Pennsylvania, United States
[4]Department of Bioengineering, University of Pittsburgh, Pittsburgh, Pennsylvania, United States

Correspondence: Michaël J. A. Girard, Ophthalmic Engineering and Innovation Laboratory, Department of Biomedical Engineering, National University of Singapore, 4 Engineering Drive 3, E4 #04-8, 117583, Singapore;
mgirard@nus.edu.sg.

Submitted: August 27, 2015
Accepted: November 25, 2015

Citation: Chung CW, Girard MJA, Jan N-J, Sigal IA. Use and misuse of Laplace's Law in ophthalmology. *Invest Ophthalmol Vis Sci*. 2016;57:236–245. DOI:10.1167/iovs.15-18053

Purpose. Laplace's Law, with its compactness and simplicity, has long been employed in ophthalmology for describing the mechanics of the corneoscleral shell. We questioned the appropriateness of Laplace's Law for computing wall stress in the eye considering the advances in knowledge of ocular biomechanics.

Methods. In this manuscript we recapitulate the formulation of Laplace's Law, as well as common interpretations and uses in ophthalmology. Using numerical modeling, we study how Laplace's Law cannot account for important characteristics of the eye, such as variations in globe shape and size or tissue thickness, anisotropy, viscoelasticity, or that the eye is a living, dynamic organ.

Results. We show that accounting for various geometrical and material factors, excluded from Laplace's Law, can alter estimates of corneoscleral wall stress as much as 456% and, therefore, that Laplace's Law is unreliable.

Conclusions. We conclude by illustrating how computational techniques, such as finite element modeling, can account for the factors mentioned above, and are thus more suitable tools to provide quantitative characterization of corneoscleral biomechanics.

Keywords: Laplace's Law, ocular biomechanics, finite element modeling, mechanical stress

The corneoscleral shell is a biomechanically resilient structure. It can withstand the external physical insults from blinking, rubbing, and atmospheric and cerebrospinal pressures.[1] It can also resist physiological alterations due to changes in intraocular pressure (IOP) and ocular pulsations.[1] Despite all these mechanical challenges, the corneoscleral shape and the relative positions of the cornea, the lens and the retina are preserved so that the visual ability is unaffected.[2–5]

Several sight-threatening pathologies are believed to be closely related to the mechanical state of the eye. For instance, certain forms of glaucoma are postulated to originate from prolonged mechanical insult to the optic nerve head (ONH) due to either elevated IOP[6] or low cerebrospinal fluid pressure.[7] Keratoconus is characterized by corneal ectasia, which leads to vision distortion, and is associated with altered corneal mechanical properties.[8] Axial myopia arises from an elongated corneoscleral shell structure such that the refracted image is not focused on the retina surface.[9,10] Overall, quantification of ocular biomechanics is paramount in advancing our understanding of ocular physiology and pathophysiology.[11] Searching the online literature repository Scopus[12] with the search terms 'eye and biomechanics' yields more than 10,000 hits from 1964 to 2013 (Fig. 1). The trend is rapidly increasing with approximately half (49.2%) of these documents being published between 2009 and 2013.

A common approach to quantify biomechanics in ophthalmology has been to employ Laplace's Law (or the Law of Laplace). Among the 97 ophthalmology journals (SCImago Journal & Country Rank),[13] 21 contained one or more manuscripts with the phrase 'Laplace's Law' or 'Law of Laplace.' Laplace's Law is an elegant mathematical approach to estimate, for thin vessels, wall stress as a function of vessel pressure, radius of container, and wall thickness. It has been applied in several areas of physiology, often used in explaining the biophysics of hollow organs, such as the alveoli[14] and the esophagus.[15] It has also been adapted to study the mechanics of the cardiac chambers.[16,17] Whereas proponents of Laplace's Law contend that it provides valuable insights to biophysical phenomena,[15,18] several authors have also written about misuse or misinterpretation in cardiovascular and respiratory biomechanics.[14,19]

As with all mathematical descriptions of physical phenomena, the Law of Laplace has several built-in assumptions that circumscribe the conditions on which it is valid. For instance, the application of Laplace's Law is limited to simple idealized pressure vessel shapes such as hollow spheres and cylinders. Furthermore, the mechanical properties of the pressure vessels are not taken into account. Violating these can lead to large errors in predictions of the mechanical behavior of biological tissues. Hence, knowledge of these limitations will benefit clinicians diagnosing ophthalmic pathologies, scientists researching in the area of ocular biomechanics, and biomedical engineers inventing new ophthalmic devices.

The purpose of this manuscript is to clarify the use of Laplace's Law in estimating stresses borne by ocular tissues. The essential biomechanical terms are first defined in Table 1. Laplace's Law is then further explained and its assumptions detailed. Subsequently, the suitability of Laplace's Law in addressing problems in ocular biomechanics is assessed. Finally, improved formulations and methodologies for predicting ocular tissue stresses are proposed.

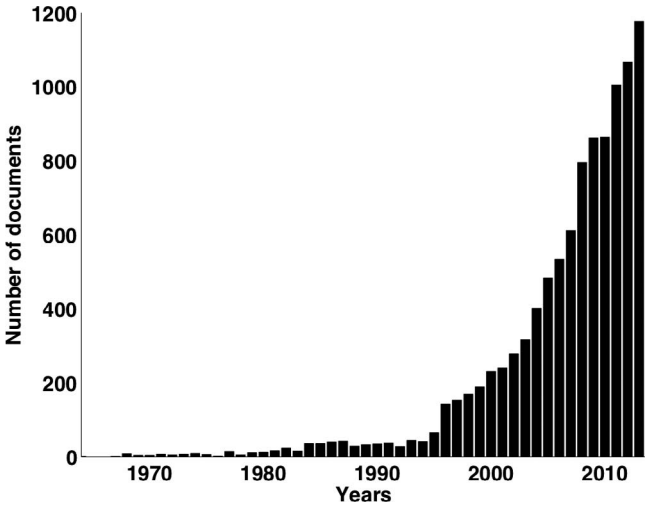

FIGURE 1. Number of documents relating to search terms 'eye and biomechanics' published from 1964 to 2013. Data from SCOPUS.[12]

LAPLACE'S LAW

Pierre-Simon, marquis de Laplace[20] (1749–1827) was a French scientist and politician (Fig. 2). He made significant contributions in mechanics, calculus, and theory of probability. In Treaty of Celestial Mechanics (Original title in French: *Traité de Mécanique Céleste*),[21] Laplace described a mathematical relationship, Laplace's Law, originally intended to quantify the liquid surface tension in a capillary.

To predict wall stress (σ), Laplace's Law can be applied to a uniform isotropic hollow sphere with thickness t and radius r, under internal pressure p (Fig. 3).[22] It is important to note that the thin shell assumption is applied in Laplace's Law, which postulates that there is no circumferential stress (stress tangential to the surface of corneoscleral shell) variation through the wall thickness. A common way to derive such a formula is to perform a balance of forces between the internal pressure (p) and the resulting wall stress. By examining the cross-section of the sphere, the total force due to the internal pressure is the product of p and the cross-sectional area (πr^2) while the aggregate circumferential tension is the product of σ, t and the cross-sectional circumference ($2\pi r$). Equating the two quantities and rearranging them leads to

$$\sigma = \frac{pr}{2t}. \quad (1)$$

When applied to the corneoscleral shell, Laplace's law is intuitive in many ways: Bigger eyes (larger r) and/or thinner corneoscleral tissue layers (smaller t) will exhibit larger wall stress. In addition, stress increases proportionally to IOP (larger p). Laplace's Law can be derived in other ways, and presented in various formulations such as using the radius of curvature instead of the spherical radius.[22] In this work we will discuss Equation 1, as it is the most commonly used formulation in ophthalmology.

TABLE 1. Essential Biomechanical Terms

Normal stress is the magnitude of force per unit area applied perpendicularly to a material cross-section. Stress can lengthen (tensile stress) or shorten (compressive stress) a given material. Three perpendicular stress components (radial, circumferential, and meridional) can be defined at any point of the corneoscleral shell surface. The SI unit of stress is Pascal (Pa).
Normal strain is a measure of material deformation as a result of stress, and can be estimated as the ratio of length change to its initial length (valid for small strain values). A positive strain implies extension, while a negative strain indicates compression. Similar to stress, three components of strain (radial, circumferential, and meridional) can be defined at any point of the corneoscleral shell. As strain is a length ratio, it is dimensionless.
Sliding of the surface of the corneoscleral shell can also results in deformations. Here, the sliding, or shear, force is applied parallel to the tissue cross-section. The shearing effect is quantified by **shear stress** and **shear strain**. The former measures the magnitude of shear force per unit of applied area in Pascal (Pa), while the later measures the angle of resulting distortion. Shear strain is dimensionless. Similar to their normal counterparts, shear stress and shear strain can be defined along the three orthogonal directions (radial, circumferential, and meridional) at any point of the corneoscleral shell.
The aggregate influence of the three normal and three shear stress components on the material can be evaluated by computing the **principal stresses**. The largest or first principal stress, and the corresponding angle indicate the maximum stress that the material undergoes and the resultant direction that it acts on. Similar measures for strain, termed **principal strains**, are calculated using the three normal and three shear strain components. The largest or first principal strain, and the respective angle suggest the maximum strain applied on the material and its direction. The principal stresses act in orthogonal directions, the same applies to the principal strains.
Von Mises stress is a single metric that can conveniently summarize the 3D state of stress. The von Mises stress is evaluated from the three principal stresses.
The elastic modulus, or **Young's modulus**, describes the elastic stiffness of a material. It is the ratio of the applied (normal) stress to its resultant (normal) strain. By evaluating the ratios of corresponding stress and strain components, the elastic modulus of a material in any direction can be assessed. The elastic modulus is measured in Pascal (Pa) and its inverse is termed compliance.
Anisotropy is the property by which materials exhibit different stiffness along different orientations. Ocular tissue is anisotropic due to its underlying collagen organization and preferred orientation. **Isotropic** materials show identical stiffness when loaded along different directions
Nonlinear materials exhibit changing stiffness with loading. Posterior scleral collagen fibers are progressively straightened with stretch, which results in tissue that is initially compliant at low load but increase in stiffness at higher load. Stiffness of nonlinear material, or its **tangent modulus**, can be deduced from the gradient of a material's stress-strain graph. Conversely, **linear** materials have constant elastic moduli.
Viscoelastic materials exhibit time-dependent stiffness determined by the rate of loading. They also dissipate energy in a loading-unloading cycle (hysteresis). Conversely, the stiffness of an **elastic** material is time-independent and energy is conserved (stored) in a loading-unloading cycle.
The mechanical properties of the corneoscleral shell are **heterogeneous**. This is contributed by location-dependent corneoscleral envelope geometry, varying tissue thickness, nonuniform underlying collagen organization, and different local tissue mechanical properties. Local stress concentrations occur at thin parts of the shell, at the limbus and regions around and in the optic nerve head.

Investigative Ophthalmology & Visual Science

Figure 2. Pierre-Simon Laplace (1749–1827). Posthumous portrait by Jean-Baptiste Paulin Guérin, 1838. (Source: Wikimedia Commons, https://commons.wikimedia.org/wiki/File:Pierre-Simon,_marquis_de_Laplace_(1745–1827)_-_Gu%C3%A9rin.jpg, {{PD-1923}}.)

Laplace's Law Is Only Valid for Thin, Hollow, and Homogeneous Spheres

In this section, we demonstrate that Laplace's Law cannot accurately predict IOP-induced wall stresses within the corneoscleral shell as the latter contains prominent morphologic irregularities.

Influence of Size and Shape

The shape of the corneoscleral shell refers to its contour and anatomical profile. The actual morphology of the corneoscleral shell is complex and irregular.[23] In humans, both the shape and the size of the corneoscleral shell vary widely among individuals and pathophysiological conditions.[23,24] Furthermore, in healthy eyes, the anterior-posterior (AP) and nasal-temporal (NT) diameters of the corneoscleral shell are approximately a millimeter longer than the superior-inferior (SI) diameter,[24] indicating that the eye is not a sphere.

How does this difference in lengths affect the computation of corneoscleral wall stress using Laplace's Law? Let's consider an example corneoscleral shell that is a perfect sphere with a diameter of 24.6 mm,[25–29] a uniform tissue thickness of 0.8 mm,[29–31] and exposed to an IOP of 2 kPa (15 mm Hg). Laplace's Law (Equation 1) predicts a circumferential stress of 15.4 kPa that is uniform over the entire shell (Fig. 4a). The situation is quite different once we consider more accurate ocular dimensions. As a case in point, consider an ellipsoidal shell with uniform thickness of 0.8 mm, with AP and NT diameters of 24.6 mm, and an SI diameter of 23.4 mm (as observed physiologically[32]). Although different formulations are available for calculating circumferential stress in nonspherical chamber,[33] we use an analytical solution developed by Regen[34] that enables us to calculate the circumferential wall stress of an ellipsoidal chamber with different diameters. The circumferential stress on the ellipsoidal shell is observed to be heterogeneous across the surface (Fig. 4b). In contrast to the result obtained from Laplace's Law, the circumferential stress peaks at the superior and inferior poles of the ellipsoidal chamber and gradually decreases toward the central transverse (AP-NT) plane. The maximum circumferential stress is 5.1% higher than the value given by Equation 1 while the minimum stress is 5.3% lower. The results indicate that Laplace's Law can both overestimate and underestimate shell stresses at different locations. Note that real corneoscleral shell shapes are more complex than the spheroid considered here, which can cause further heterogeneity in stress fields.[35,36]

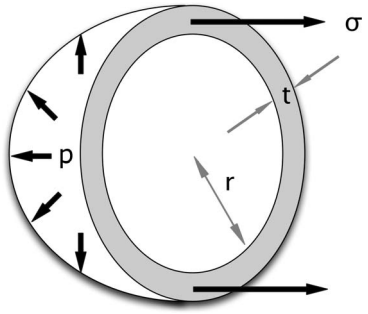

Figure 3. Derivation of Laplace's Law. The equation is derived by balancing the forces due to internal pressure (p) and circumferential stress (σ) for a spherical shell of radius (r) and thickness (t).

Errors from Laplace's law can increase considerably when considering pathophysiological conditions. For instance, axial myopia can lead to 7.5% lengthening of the axial length compared with emmetropic eyes.[10,37] Our analysis suggests that if the axial length extends from 24.6 to 26.4 mm (equivalent to a mild myopia case of −5.07 diopters [D][38]), the maximum stress is 12.2% higher than that computed by Laplace's law, while the minimum stress would be 11.8% lower (Fig. 4c). As the various axes of the spheroids are different, the range of differences in stresses will increase. In the case of severe axial myopia, the axial diameter can exceed 33.5 mm (approximately −25.01 D),[39] the errors can escalate to 31.3% and 30.7%. The stress distribution also reveals regions of higher stress concentration compared with the healthy eye, particularly at the superior and inferior poles. These localized areas of high stress could potentially be susceptible to material rupture.

Geometrical discontinuities within the corneoscleral shell also make the use of Laplace's Law inappropriate. In humans, the protrusion of the cornea is characterized by a change in shell curvature at the limbus, resulting in limbal stress concentrations. The maximum von Mises stress (Table 1) at the limbus is estimated to be four times that in the cornea, and 30% higher than that in the sclera.[36] Furthermore, distinct curvatures, thicknesses, porosities, and microstructures between the peripapillary sclera and the neighboring lamina cribrosa (LC) grant the postulation of Laplace inadmissible.[40,41] A study has shown that the abrupt change in geometrical and mechanical properties at the scleral canal boundary could lead to an acute stress concentration in the ONH region of up to 25 times the value of IOP.[42] The quantity is 300% higher than that estimated through Laplace's Law, yet the latter is still commonly used to predict ONH stresses.

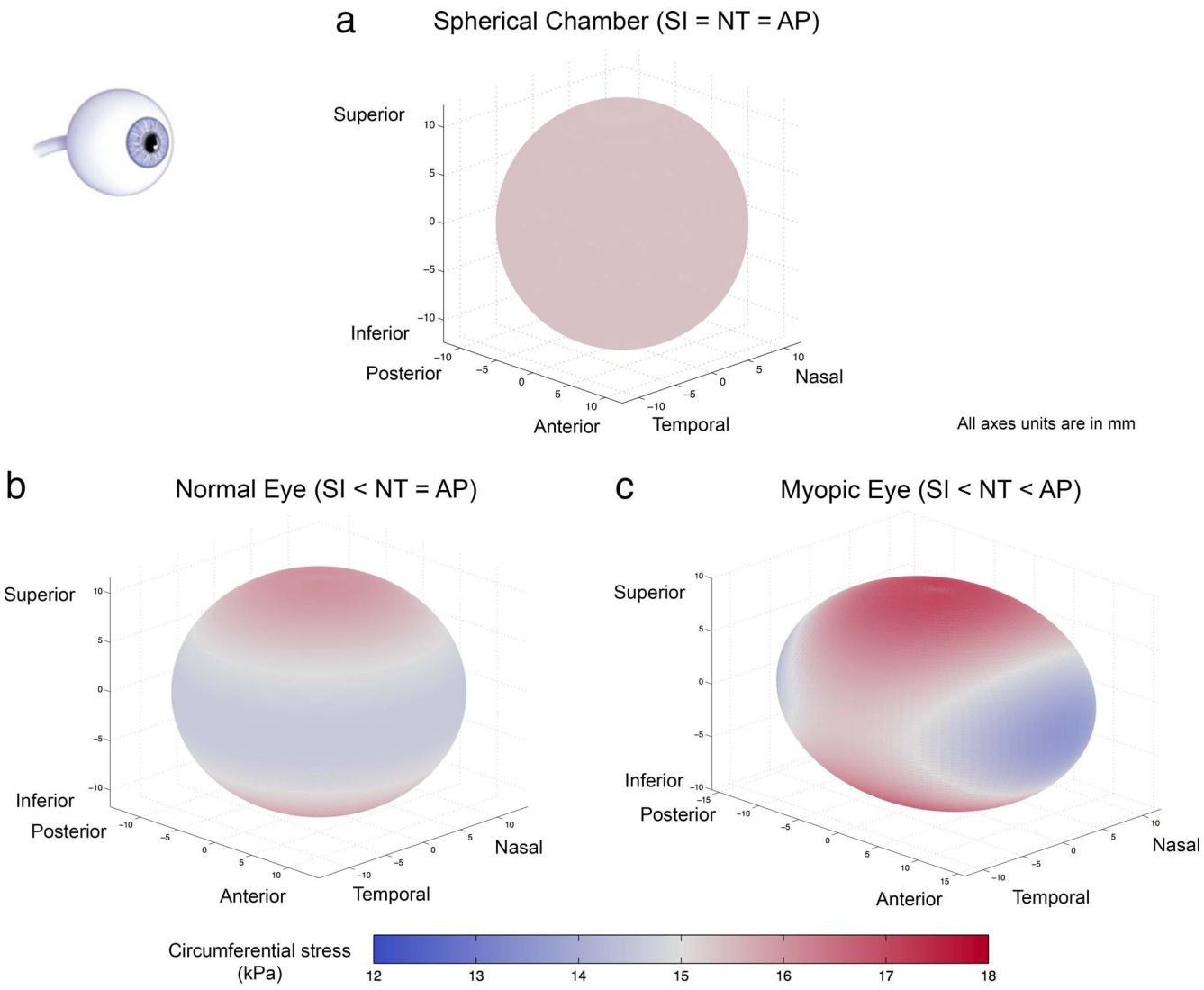

Figure 4. Circumferential stress color maps of a spherical chamber, a normal eye and a myopic eye (represented as ellipsoidal chambers), as predicted by the Regen's formulation.[34] The chambers are oriented according to the eyeball on the *top left*. Each shell has a thickness of 0.8 mm and an IOP of 2 kPa (15 mm Hg). (**a**) The spherical shell has a diameter of 24.6 mm, and a uniform circumferential stress of 15.4 kPa. The result is identical to that of Laplace's Law. (**b**) In the case of a normal eye, the SI axis is shorter than the AP and NT axes (23.4 vs. 24.6 mm). The model suggests that both the superior and inferior poles experience the maximum circumferential stress. (**c**) In a myopic eye, the SI axis is shorter than the NT axis, which in turn shorter than the AP axis (23.4 vs. 24.6 vs. 26.4 mm). According to the model, superior/inferior pole experiences the maximum circumferential stress while the anterior/posterior pole undergoes the minimum stress value. In (**b**) and (**c**), the differences between axial lengths are magnified ×4 for illustration purposes.

Overall, Laplace's Law, with its assumption of constant radius, cannot produce the circumferential stress variation due to unequal axial length and anatomical features.

Influence of Tissue Thickness

The thickness of the corneoscleral shell is location-dependent.[29,35,43] The corneal thickness is approximately 520 μm near the center and increases toward the peripheral region (~660 μm).[44] In the sclera, starting from the limbus and traversing posteriorly, the average thickness decreases monotonically until it reaches a minimum near the equator, where the tissue begins to increase in thickness toward the posterior pole. At the ONH, the scleral tissue tapers toward the scleral canal.[5,43] The sclera does not have a constant thickness along both NT and SI directions. Peripapillary scleral thickness varies, being thinnest at the inferior and nasal quadrants (~880 μm), and thickest at the superior and temporal quadrants (~1050 μm).[43] The heterogeneity of corneoscleral tissue thickness can adversely affect the approximation made from Laplace's Law. The thinner parts of the shell can exhibit higher IOP-induced stress than the thicker parts due to a smaller cross-sectional area. Variations in corneoscleral shell thickness, ranging from around 100 μm at the thinnest, to over 1000 μm at the thickest, would imply also an order of magnitude in variations in local stress.[45] This stress heterogeneity cannot be predicted by Laplace's Law.

Ophthalmic disorders can also result in considerable changes in the ratio of corneoscleral shell thickness to eye globe diameter. For instance, hyperopia is related to both increased scleral thickness and reduced axial diameter.[44,46] The increased thickness-to-diameter proportion can yield larger stress difference between the inner and outer surfaces; the thin shell assumption from Laplace is no

Table 2. Comparison of Laplace's Law and Recent FE Models Considerations

Model (Physiological Focus)	Geometrical Considerations		Material Considerations			
	Shape	Thickness	Anisotropy	Nonlinearity	Viscoelasticity	Inhomogeneity
Laplace's Law[21]	•	•	⊘	⊘	⊘	⊘
Woo et al.[56] (CS)	•	★	•	★	•	•
Bellezza et al.[81] (ONH) Asejczyk-Widlicka et al.[82] (CS) Sigal et al.[42] (ONH/LC)	•	•	•	•	•	•
Pinsky et al.[58] (CS) Zhang et al.[75] (ONH/LC)	•	•	★	★	•	★
Sigal et al.[83] (ONH/LC) Sigal et al.[84] (ONH/LC)	★	★	•	•	•	•
Roberts et al.[86] (CS/LC)	★	★	★	•	•	•
Girard et al.[35] (CS) Grytz et al.[57] (CS/LC) Coudrillier et al.[60] (CS/ONH) Coudrillier et al.[85] (CS)	★	★	★	★	•	★
Asejczky-Widlicka et al.[50] (CS)	★	★	•	★	•	•
Norman et al.[23] (CS/ONH)	•	★	•	•	•	•
Perez et al.[36] (CS)	★	★	•	•	★	•

Region of focus: Corneoscleral shell (CS); lamina cribrosa (LC); optic nerve head (ONH).
Shape: Idealized spherical, ellipsoidal or hybrid shell (•); anatomical shape of mammalian eye (★).
Thickness: Uniform (•); anatomical (★).
Anisotropy: Isotropic (•); anisotropic (★); not applicable (⊘).
Nonlinearity: Linear (•); nonlinear (★); not applicable (⊘).
Viscoelasticity: Elastic or hyperelastic (•); viscoelastic (★); not applicable (⊘).
Inhomogeneity: Homogeneous (•); inhomogeneous (★); not applicable (⊘).

longer valid. In fact, the circumferential stress (across the corneoscleral tissue) is better represented from the thick shell theory.[22] The thick shell theory accounts for the pressure difference across the wall and recognizes the variation of circumferential wall stress across the wall thickness. We assume that the IOP is applied on the inner surface with zero external pressure. In this case, the maximum circumferential stress occurs at the inner surface while the minimum at the outer surface. Considering a healthy eye globe with an axial diameter of 24.6 mm and a wall thickness of 0.8 mm (thickness-to-radius ratio of 0.03), the circumferential wall stress obtained from Laplace's Law is 3.3% lower than the maximum stress value and 3.3% higher than the minimum stress value evaluated from the thick shell equation.[22] In the case of hyperopia with axial diameter of 17.2 mm[44] and wall thickness of 0.8 mm, (thickness-to-radius ratio of 0.047), the differences from the inner wall circumferential stress and the outer wall stress rise to 4.6% and 4.7%, respectively.

Overall, Laplace's Law, with its assumption of uniform stress across the wall, can produce unreliable results when it is applied to compute the circumferential stress of the eye with varying and thick scleral tissue.[35]

Corneoscleral Shell Mechanical Properties Are Not Accounted for in Laplace's Law

In this section, we illustrate that the exclusion of corneoscleral tissue mechanical properties within Laplace's law can lead to vastly inaccurate approximations of wall stress. Unfortunately, deriving analytical, closed form solutions that can account for complex tissue mechanical properties remains impossible. Thus, we will compare predictions of stress made with Laplace's Law with those made numerically, namely using finite element (FE) modeling.

Computational Modeling of Corneoscleral Tissue Microstructure

Apart from its geometrical features, the corneoscleral shell varies in mechanical properties by location and by depth. The stroma is the main load-bearing layer, which is reinforced by collagen fibrils of different sizes, organizations, alignments, and preferred orientations. The scleral stroma contains mainly Type 1 collagen, whose diameter and compactness increases with tissue depth.[47] Collagen fibrils in the corneal stroma are thin and highly organized.[48] The collagen fibers form rings surrounding the limbus that reinforce the region near the cornea.[49] The collagenous microstructure of the corneoscleral shell contributes to its unique mechanical characteristics including anisotropy, nonlinearity, viscoelasticity, and inhomogeneity.

As for complex shapes, Laplace's Law cannot account for complex mechanical properties. To overcome such a limitation, investigators have attempted to couple Laplace's Law with stress-strain relationships derived from cadaverous corneoscleral tissues,[50] modify Laplace's Law to accommodate varying curvatures,[33] or build finite element models incorporating complex geometrical and material features as those described in Table 2.

In the following sections, we investigate the influences of anisotropy, viscoelasticity, heterogeneity, and nonlinearity on circumferential stress calculations using FE modeling. We also compare the Laplace's Law results with FE computations, where applicable.

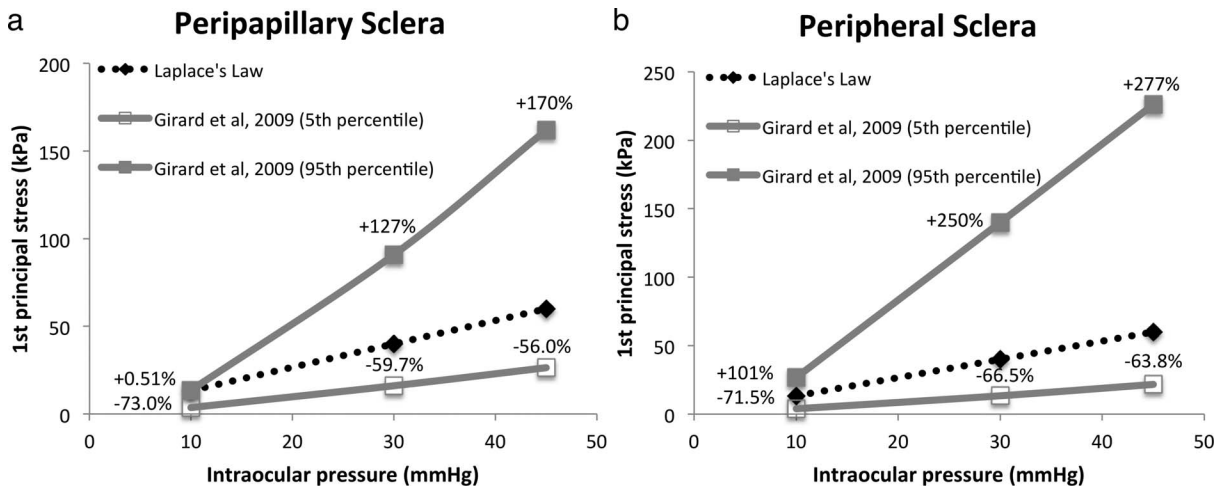

Figure 5. Stress of FE model of monkey[35] (**a**) peripapillary sclera and (**b**) peripheral sclera and those of Laplace's Law. Percentage differences between the FE and Laplace's Law stress values are indicated. Dimensions of spherical thin shell for Laplace's Law evaluation: thickness 0.5 mm, radius 10 mm.

Influence of Anisotropy

The fibrils underlying the corneoscleral tissue can provide extra stiffness during deformation. As the majority of the underlying collagen fibers lie within a plane parallel to the shell surface,[51] the corneoscleral layer is stiffer along the tangential direction, and is thus well adapted to resist IOP-induced stress. The anterior sclera immediately adjacent to the limbus and the peripapillary sclera that surrounds the optic disc, both exhibit high anisotropy with circumferential organizations.[49] Such microstructural organizations are thought to provide reinforcements in order to limit corneal and ONH deformations.[52] The varying fiber arrangements are related to change in circumferential stress that cannot be explained by Laplace's Law.[45]

To understand the consequences of applying Laplace's Law to a region with high material anisotropy, we compared the wall stress obtained from a monkey posterior scleral FE model[35] with that from a spherical vessel of similar size computed with Laplace's Law. We focus our comparisons to the peripapillary sclera, a relatively high anisotropic region. Note that the stress estimates from the FE model were obtained based on an anatomically-accurate scleral shell geometry, three-dimensional (3D) experimental deformation measurements, and a realistic constitutive model that took into account collagen fiber anisotropy. Such stresses can be considered more reliable for the monkey eye than those from Laplace's Law.

From the FE model, the 95th percentile stress (first principal) in the peripapillary sclera at 10 mm Hg was 0.51% higher than that estimated from Laplace's Law while the 5th percentile stress was 73% less (Fig. 5a). The values at 5% and 95% represent the minimum stress and maximum stress in the FE computation after eliminating the outliners. Differences worsened when IOP was increased to 30 mm Hg (127% and −59.7%) and 45 mm Hg (170% and −56.0%). In sum, Laplace's Law is incapable of incorporating the direction-dependent biomechanical features of the corneoscleral shell, and thus cannot predict the effects of underlying collagen fiber orientations on wall stress in the peripapillary sclera.

Influence of Viscoelasticity

The corneoscleral shell is viscoelastic, with mechanical properties that vary with loading rates. Studies showed that mammalian cornea[53] and scleral[54] tissues stiffness increases with tissue loading speed. Corneoscleral tissue viscoelasticity is also characterized by the energy dissipated during loading-unloading cycles, defined as hysteresis.[53,54] The phenomena of rate-dependent stiffness and hysteresis are postulated to help ocular tissues dissipate the deformation energy and protect them from sudden loading and excessive deformation, such as in blast trauma, in order to prevent injury.

Perez and colleagues[36] developed a viscoelastic FE model of the corneoscleral shell to simulate the effect of in vitro PBS injection in expanding ocular volume and elevating IOP. They demonstrated greater and more rapid IOP increases at faster injection rates, as a result of tissue viscoelasticity inducing larger instantaneous tissue stiffness. Volumetric injections of 15 μL at slow (0.1 μLs^{-1}) and intermediate (1.5 μLs^{-1}) rates could lead to IOP changes (in their model) of 8 and 11 mm Hg, respectively. In the case of a fast injection (15 μLs^{-1}), an IOP change of 14 mm Hg was reported, while von Mises stress ranged from 3.74 kPa (5th percentile) to 18.4 kPa (95th percentile). In fact, the distribution of von Mises stress (calculated from the principal stresses) computed from the viscoelastic FE model contrasts with the stress value produced by Laplace's Law, which is evaluated to be 20.8 kPa at IOP of 14 mm Hg (456% and 13.0% higher than the 5th and 95th percentile stress values predicted from viscoelastic FE models, respectively). In addition, Laplace's Law cannot be used to calculate the change of circumferential wall stress due to a change in IOP, as the rate of change of IOP can affect the instantaneous stiffness of the corneoscleral tissue and its deformation. In sum, Laplace's Law cannot be used to make predictions that consider the effect of viscoelasticity.

Influence of Heterogeneity

The mechanical properties of fiber-reinforced corneoscleral shell are direction-dependent (anisotropy), strain-dependent (nonlinearity), and rate-dependent (viscoelasticity). As collagen deposition, alignment direction, and organization varies in different regions[49] and at different tissue depth,[51,55] the local mechanical properties are also location-dependent (heterogeneity). Laplace's law is unable to take such complexities into account, and caution should be taken when estimating wall stresses (e.g., in different regions of the scleral shell. In the latter, strong variations in biomechanical properties exist among the anterior, equatorial, and posterior regions).[54]

Influence of Nonlinearity

It has been repeatedly demonstrated that the tissues of the eye stiffen with stretch,[45,54,56] exhibiting a nonlinear relationship between circumferential stress and IOP. This is because, as stretch increases with IOP, more and more collagen fibers uncrimp, or straighten, and become recruited to resist the increasing load.[35,57–59] Laplace's law does not intrinsically presuppose a linear relationship between stretch and stress. Hence, as long as other assumptions are satisfied, (i.e., a perfect thin spherical shell that is homogeneous and isotropic) Laplace's Law would apply equally well when the material is linear or nonlinear. However, any deviation from these conditions would cause Laplace's Law assumptions to be violated and lead to invalid predictions. Consider, for example, a spherical shell made of a material that is homogeneous, isotropic and nonlinear, with small variations in shell thickness. As IOP increases the stresses on the wall deform the material. In regions where the shell is thinner, the stresses will be slightly higher, which leads to a slightly stiffer material locally.[45] In this way, the inhomogeneity in shell thicknesses has been translated into material inhomogeneity.

To demonstrate the shortcoming of Laplace's law as a result of excluding material nonlinearity in its estimation, we compared the wall stress obtained from the aforementioned monkey posterior scleral FE model[35] with that from a spherical vessel of similar size computed with Laplace's Law. We focus our comparisons to the peripheral sclera (surrounding the scleral canal and further than 1.7 mm from the canal), because it is less anisotropic than other regions of the eye.[49,60] The stress data produced from the model deviate from the calculated stress using Laplace's Law and the difference increases with the pressure. The 95th percentile of first principal stress within the peripheral monkey sclera at 10 mm Hg is predicted to be 101% higher than the Laplace's Law wall stress while the 5th percentile of the stress is 71.5% lower. The errors escalate to 250% and –66.5% for 30 mm Hg, and 277% and –63.8% for 45 mm Hg, respectively (Fig. 5b). The comparison shows that the usage of Laplace's Law to estimate the circumferential wall stress can lead to large error as a result of not accounting for material nonlinearity.

Special Considerations: The Eye Is a Living, Dynamic System

Finally, Laplace's Law is not suitable for evaluating corneoscleral biomechanics because it assumes the eye globe as a nonadaptive and passive mechanical chamber. Instead, the eye continuously adapts (remodels) in response to physiological needs, external physical factors, aging, and diseased conditions thought to be intended to maintain a homeostatic state.[61,62] In addition, the observed presence of contractile cells (myofibroblasts) within the scleral shell could provide the eye with an additional mechanism to alter its elasticity (and thus its stress levels). The adaptive and active behaviors of the scleral shell (unaccounted for in Laplace's law) are briefly described below.

Adaptive Scleral Behavior: Remodeling in Myopia and Glaucoma

In myopia, it has been hypothesized that the scleral fibroblasts, which govern collagen and proteoglycan production, have a regulatory role in the scleral thinning process.[63] The changed scleral material composition and increased laminar architecture[64] may lead to a higher probability of scleral interlayer sliding, thus increasing creep[65] (faster and larger scleral stretch under load). In glaucoma or in response to chronic IOP elevations, studies have reported scleral thinning,[66] structural scleral stiffening,[45] and changes in scleral collagen fiber orientation.[67] While Laplace's law may be able to consider simplistic remodeling conditions (through changes in shell thickness and/or eye radius), it is unable to account for complex remodeling conditions observed in both myopia and glaucoma.

Active Scleral Behavior: Evidence for Contractile Activity

Alpha-smooth muscle actin (often expressed in myofibroblasts) has been found in some scleral cells.[64,68] Such myofibroblast-like cells may be able to alter the biomechanical properties of the sclera through contractile activity.[69] The presence of myofibroblasts in tree shrew sclera helped to curb the eye expansion rate after increasing IOP from 15 to 100 mm Hg, and to returned to its pre-expansion shape within an hour. Results from other in vitro studies[69,70] suggested that scleral fibroblasts could be differentiated into myofibroblasts through cytokine TGF-β.[68,70] Laplace's law, as formulated, can only predict passive stress, and would be unable to take into account active stress as generated by scleral myofibroblasts.

Merits of Laplace's Law in Ophthalmology

Despite its limitations, Laplace's Law is a useful tool in ophthalmology. Laplace's Law summarizes the interaction of physical variables and illustrates intuitive concepts of stress in corneoscleral tissues. The popular law is a basis for communications among scientists, engineers and clinicians in diverse fields of ophthalmology and facilitates the exchange of ideas. Laplace's Law is also useful for educating engineering students and clinicians about the physics of the eye and complex biomechanical concepts.

We recognize that Laplace's Law is attractive because it is simple and easy to use, and that sometimes it will produce useful estimates. However, in a real eye Laplace's Law will never be exact, and therefore those who use it have the responsibility to demonstrate that the approximation is good enough for their use.

Discussion

The limitations of Laplace's Law are reflected in its partial or nonconsideration of geometrical and material factors in explaining the biomechanics of the corneoscleral envelope. Paradoxically, these assumptions facilitate the formulation of a simple, clear, and compact relation between IOP and wall stress. While Laplace's Law offers a gross first approximation of IOP-induced wall stress, it can produce vastly inaccurate estimates, and more accurate methods are demanded for better understanding of the complex physiology and pathophysiology of the eye.

Finite element modeling of the corneoscleral shell is promising. Features such as anatomically-accurate shape and thickness,[23] nonlinear mechanical properties,[35,71] collagen microstructural descriptions,[35,71,72] and growth and remodeling[57] have been considered in these models. However, FE models have their own limitations as well, and validations of these models are still needed. Recent usage of x-ray scattering,[60,73] small angle light scattering,[49,74–76] and polarized light microscopy[59] to decipher the collagen arrangement will enhance the accuracy of the models.[49] Implementations of linear,[36] and probably nonlinear[77,78] viscoelastic models in simulation can also advance sophistication and quality of simulation over time. The use of inverse FE methods[35,53,60] or

prefitting techniques[79] may help bridge the gap between experimental data and simulation results and provide advantages for clinical translations.

The main draw of Laplace's Law is its simplicity. Finite element models can also be simple and user-friendly, as Sigal[80] has developed an applet for simple FE modeling of the ONH. The work provides an alternative avenue to understanding the biomechanics of the eye without being limited by technical knowledge.

Laplace never meant to model the eye, and we should exercise caution in using the famous law.

Acknowledgments

Supported by grants from the Ministry of Education Academic Research Funds, Tier 1 (MJAG; R-397-000-181-112; Singapore) and from an NUS Young Investigator Award (MJAG; NUSYIA_FY13_P03, R-397-000-174-133; Singapore), the donors of the NGR, a program of the BrightFocus Foundation (formerly American Health Assistance Foundation or AHAF; Clarksburg, MD, USA), and from the National Institutes of Health NIH R01EY023966 and R01EY025011 (IAS and NJJ; Bethesda, MD, USA).

Disclosure: **C.W. Chung**, None; **M.J.A. Girard**, None; **N.-J. Jan**, None; **I.A. Sigal**, None

References

1. Ethier CR, Johnson M, Ruberti J. Ocular biomechanics and biotransport. *Annu Rev Biomed Eng*. 2004;6:249–273.
2. Jonas JB, Holbach L, Panda-Jonas S. Scleral cross section area and volume and axial length. *PLoS One*. 2014;9:e93551.
3. Asejczyk-Widlicka M, Srodka DW, Kasprzak H, Pierscionek BK. Modelling the elastic properties of the anterior eye and their contribution to maintenance of image quality: the role of the limbus. *Eye*. 2007;21:1087–1094.
4. Anderson K, El-Sheikh A, Newson T. Application of structural analysis to the mechanical behaviour of the cornea. *Soc Interface*. 2004;1:3–15.
5. Vurgese S, Panda-Jonas S, Jonas JB. Scleral thickness in human eyes. *PLoS One*. 2012;7:e29692.
6. Sigal IA, Flanagan JG, Ethier CR. Factors influencing optic nerve head biomechanics. *Invest Ophthalmol Vis Sci*. 2005; 46:4189–4199.
7. Ren R, Jonas JB, Tian G, et al. Cerebrospinal fluid pressure in glaucoma: a prospective study. *Ophthalmology*. 2010;117: 259–266.
8. Romero-Jimenez M, Santodomingo-Rubido J, Wolffsohn JS. Keratoconus: a review. *Cont Lens Anterior Eye*. 2010;33:157–166, quiz 205.
9. McBrien NA, Gentle A. Role of the sclera in the development and pathological complications of myopia. *Prog Retin Eye Res*. 2003;22:307–338.
10. Greene PR. Mechanical considerations in myopia: relative effects of accommodation, convergence, intraocular pressure, and the extraocular muscles. *Am J Opt Physiol Optics*. 1980; 57:902–914.
11. Girard MJ, Dupps WJ, Baskaran M, et al. Translating ocular biomechanics into clinical practice: current state and future prospects. *Curr Eye Res*. 2015;40:1–18.
12. Scopus. Elsevier. Available at http://www.scopus.com. Accessed February 16, 2015.
13. SCImago. SJR—SCImago Journal & Country Rank; 2007. Available at: http://www.scimagojr.com. Accessed December 13, 2013.
14. Prange HD. Laplace's law and the alveolus: a misconception of anatomy and a misapplication of physics. *Adv Physiol Educ*. 2003;27:34–40.
15. Basford JR. The Law of Laplace and its relevance to contemporary medicine and rehabilitation. *Arch Phys Med Rehab*. 2002;83:1165–1170.
16. Li JK. Comparative cardiac mechanics: Laplace's Law. *J Theor Biol*. 1986;118:339–343.
17. Martin RR, Haines H. Application of Laplace's law to mammalian hearts. *Comp Biochem Physiol*. 1970;34:959–962.
18. Wolf AV. Demonstration concerning pressure-tension relations in various organs. *Science*. 1952;115:243–244.
19. Valentinuzzi ME, Kohen AJ, Zanutto BS. Laplace's law. Its epistemological context. *IEEE Pulse*. 2011;2:71–76.
20. Gillispie CC, Fox R, Grattan-Guinness I. *Pierre-Simon Laplace, 1749-1827: A Life in Exact Science*. Princeton: Princeton University Press; 1997.
21. Laplace PS. *Académie des sciences (France). Œuvres complètes de Laplace, publiées sous les auspices de l'Académie des sciences*. Paris: Gauthier-Villars; 1878.
22. Fung YC. *Biomechanics: Mechanical Properties of Living Tissues*. 2nd ed. New York: Springer-Verlag; 1993.
23. Norman RE, Flanagan JG, Sigal IA, Rausch SM, Tertinegg I, Ethier CR. Finite element modeling of the human sclera: influence on optic nerve head biomechanics and connections with glaucoma. *Exp Eye Res*. 2011;93:4–12.
24. Singh KD, Logan NS, Gilmartin B. Three-dimensional modeling of the human eye based on magnetic resonance imaging. *Invest Ophthalmol Vis Sci*. 2006;47:2272–2279.
25. Jonas JB, Berenshtein E, Holbach L. Anatomic relationship between lamina cribrosa, intraocular space, and cerebrospinal fluid space. *Invest Ophthalmol Vis Sci*. 2003;44:5189–5195.
26. Jonas JB, Berenshtein E, Holbach L. Lamina cribrosa thickness and spatial relationships between intraocular space and cerebrospinal fluid space in highly myopic eyes. *Invest Ophthalmol Vis Sci*. 2004;45:2660–2665.
27. Jonas JB, Mardin CY, Schlotzer-Schrehardt U, Naumann GO. Morphometry of the human lamina cribrosa surface. *Invest Ophthalmol Vis Sci*. 1991;32:401–405.
28. Jonas JB, Stroux A, Velten I, Juenemann A, Martus P, Budde WM. Central corneal thickness correlated with glaucoma damage and rate of progression. *Invest Ophthalmol Vis Sci*. 2005;46:1269–1274.
29. Olsen TW, Aaberg SY, Geroski DH, Edelhauser HF. Human sclera: thickness and surface area. *Am J Ophthalmol*. 1998; 125:237–241.
30. Downs JC, Blidner RA, Bellezza AJ, Thompson HW, Hart RT, Burgoyne CF. Peripapillary scleral thickness in perfusion-fixed normal monkey eyes. *Invest Ophthalmol Vis Sci*. 2002;43: 2229–2235.
31. Downs JC, Ensor ME, Bellezza AJ, Thompson HW, Hart RT, Burgoyne CF. Posterior scleral thickness in perfusion-fixed normal and early-glaucoma monkey eyes. *Invest Ophthalmol Vis Sci*. 2001;42:3202–3208.
32. Ruete CGT. Ocular physiology. *Strabismus*. 1999;7:43–60.
33. Coudrillier B, Tian J, Alexander S, Myers KM, Quigley HA, Nguyen TD. Biomechanics of the human posterior sclera: age- and glaucoma-related changes measured using inflation testing. *Invest Ophthalmol Vis Sci*. 2012;53:1714–1728.
34. Regen DM. Tensions and stresses of ellipsoidal chambers. *Ann Biomed Eng*. 1996;24:400–417.
35. Girard MJA, Downs JC, Bottlang M, Burgoyne CF, Suh JK. Peripapillary and posterior scleral mechanics–part II: experimental and inverse finite element characterization. *J Biomed Eng*. 2009;131:051012.
36. Perez BC, Morris HJ, Hart RT, Liu J. Finite element modeling of the viscoelastic responses of the eye during microvolumetric changes. *J Biomed Sci Eng*. 2013;6:29–37.
37. McBrien NA, Adams DW. A longitudinal investigation of adult-onset and adult-progression of myopia in an occupational

group. Refractive and biometric findings. *Invest Ophthalmol Vis Sci*. 1997;38:321–333.

38. Olsen T. Sources of error in intraocular lens power calculation. *J Cataract Refract Surg*. 1992;18:125–129.
39. Curtin BJ, Karlin DB. Axial length measurements and fundus changes of the myopic eye. *Am J Ophthalmol*. 1971;71:42–53.
40. Roberts MD, Grau V, Grimm J, et al. Remodeling of the connective tissue microarchitecture of the lamina cribrosa in early experimental glaucoma. *Invest Ophthalmol Vis Sci*. 2009;50:681–690.
41. Thakku SG, Tham YC, Baskaran M, et al. A global shape index to characterize anterior lamina cribrosa morphology and its determinants in healthy Indian eyes. *Invest Ophthalmol Vis Sci*. 2015;56:3604–3614.
42. Sigal IA, Flanagan JG, Tertinegg I, Ethier CR. Finite element modeling of optic nerve head biomechanics. *Invest Ophthalmol Vis Sci*. 2004;45:4378–4387.
43. Norman RE, Flanagan JG, Rausch SM, et al. Dimensions of the human sclera: thickness measurement and regional changes with axial length. *Exp Eye Res*. 2010;90:277–284.
44. Martola EL, Baum JL. Central and peripheral corneal thickness. A clinical study. *Arch Ophthalmol*. 1968;79:28–30.
45. Girard MJ, Suh JK, Bottlang M, Burgoyne CF, Downs JC. Biomechanical changes in the sclera of monkey eyes exposed to chronic IOP elevations. *Invest Ophthalmol Vis Sci*. 2011;52:5656–5669.
46. Cheng HM, Singh OS, Kwong KK, Xiong J, Woods BT, Brady TJ. Shape of the myopic eye as seen with high-resolution magnetic resonance imaging. *Optom Vis Sci*. 1992;69:698–701.
47. Levin LA, Kaufman PL. *Adler's Physiology of the Eye: Clinical Application.* 11th ed. Edinburgh: Saunders/Elsevier; 2011.
48. Boote C, Kamma-Lorger CS, Hayes S, et al. Quantification of collagen organization in the peripheral human cornea at micron-scale resolution. *Biophys J*. 2011;101:33–42.
49. Girard MJ, Dahlmann-Noor A, Rayapureddi S, et al. Quantitative mapping of scleral fiber orientation in normal rat eyes. *Invest Ophthalmol Vis Sci*. 2011;52:9684–9693.
50. Asejczyk-Widlicka M, Srodka W, Schachar RA, Pierscionek BK. Material properties of the cornea and sclera: a modelling approach to test experimental analysis. *J Biomech*. 2011;44:543–546.
51. Komai Y, Ushiki T. The three-dimensional organization of collagen fibrils in the human cornea and sclera. *Invest Ophthalmol Vis Sci*. 1991;32:2244–2258.
52. Amini R, Barocas VH. Anterior chamber angle opening during corneoscleral indentation: the mechanism of whole eye globe deformation and the importance of the limbus. *Invest Ophthalmol Vis Sci*. 2009;50:5288–5294.
53. Boyce BL, Jones RE, Nguyen TD, Grazier JM. Stress-controlled viscoelastic tensile response of bovine cornea. *J Biomech*. 2007;40:2367–2376.
54. Elsheikh A, Geraghty B, Alhasso D, Knappett J, Campanelli M, Rama P. Regional variation in the biomechanical properties of the human sclera. *Exp Eye Res*. 2010;90:624–633.
55. Danford FL, Yan D, Dreier RA, Cahir TM, Girkin CA, Vande Geest JP. Differences in the region- and depth-dependent microstructural organization in normal versus glaucomatous human posterior sclerae. *Invest Ophthalmol Vis Sci*. 2013;54:7922–7932.
56. Woo SL, Kobayashi AS, Schlegel WA, Lawrence C. Nonlinear material properties of intact cornea and sclera. *Exp Eye Res*. 1972;14:29–39.
57. Grytz R, Meschke G, Jonas JB. The collagen fibril architecture in the lamina cribrosa and peripapillary sclera predicted by a computational remodeling approach. *Biomech Model Mechanobiol*. 2011;10:371–382.
58. Pinsky PM, van der Heide D, Chernyak D. Computational modeling of mechanical anisotropy in the cornea and sclera. *J Cataract Refract Surg*. 2005;31:136–145.
59. Jan NJ, Grimm JL, Tran H, et al. Polarization microscopy for characterizing fiber orientation of ocular tissues. *Biomed Opt Express*. 2015;6:4705–4718.
60. Coudrillier B, Boote C, Quigley HA, Nguyen TD. Scleral anisotropy and its effects on the mechanical response of the optic nerve head. *Biomech Model Mechanobiol*. 2013;12:941–963.
61. Sigal IA, Bilonick RA, Kagemann L, et al. The optic nerve head as a robust biomechanical system. *Invest Ophthalmol Vis Sci*. 2012;53:2658–2667.
62. Artal P, Benito A, Tabernero J. The human eye is an example of robust optical design. *J Vis*. 2006;6(1):1–7.
63. Jobling AI, Nguyen M, Gentle A, McBrien NA. Isoform-specific changes in scleral transforming growth factor-beta expression and the regulation of collagen synthesis during myopia progression. *J Biol Chem*. 2004;279:18121–18126.
64. McBrien NA, Jobling AI, Gentle A. Biomechanics of the sclera in myopia: extracellular and cellular factors. *Optom Vis*. 2009;86:E23–E30.
65. Phillips JR, Khalaj M, McBrien NA. Induced myopia associated with increased scleral creep in chick and tree shrew eyes. *Invest Ophthalmol Vis Sci*. 2000;41:2028–2034.
66. Yang H, Downs JC, Girkin C, et al. 3-D histomorphometry of the normal and early glaucomatous monkey optic nerve head: lamina cribrosa and peripapillary scleral position and thickness. *Invest Ophthalmol Vis Sci*. 2007;48:4597–4607.
67. Pijanka JK, Coudrillier B, Ziegler K, et al. Quantitative mapping of collagen fiber orientation in non-glaucoma and glaucoma posterior human sclerae. *Invest Ophthalmol Vis Sci*. 2012;53:5258–5270.
68. Jobling AI, Gentle A, Metlapally R, McGowan BJ, McBrien NA. Regulation of scleral cell contraction by transforming growth factor-beta and stress: competing roles in myopic eye growth. *J Biol Chem*. 2009;284:2072–2079.
69. Phillips JR, McBrien NA. Pressure-induced changes in axial eye length of chick and tree shrew: significance of myofibroblasts in the sclera. *Invest Ophthalmol Vis Sci*. 2004;45:758–763.
70. Vaughan MB, Howard EW, Tomasek JJ. Transforming growth factor-beta1 promotes the morphological and functional differentiation of the myofibroblast. *Exp Cell Res*. 2000;257:180–189.
71. Girard MJA, Downs JC, Burgoyne CF, Suh JK. Peripapillary and posterior scleral mechanics–part I: development of an anisotropic hyperelastic constitutive model. *J Biomed Eng*. 2009;131:051011.
72. Gouget CL, Girard MJ, Ethier CR. A constrained von Mises distribution to describe fiber organization in thin soft tissues. *Biomech Model Mechanobiol*. 2012;11:475–482.
73. Boote C, Dennis S, Meek K. Spatial mapping of collagen fibril organisation in primate cornea-an X-ray diffraction investigation. *J Struct Biol*. 2004;146:359–367.
74. Yan D, McPheeters S, Johnson G, Utzinger U, Vande Geest JP. Microstructural differences in the human posterior sclera as a function of age and race. *Invest Ophthalmol Vis Sci*. 2011;52:821–829.
75. Zhang L, Albon J, Jones H, et al. Collagen microstructural factors influencing optic nerve head biomechanics. *Invest Ophthalmol Vis Sci*. 2015;56:2031–2042.
76. Jones HJ, Girard MJ, White N, et al. Quantitative analysis of three-dimensional fibrillar collagen microstructure within the normal, aged and glaucomatous human optic nerve head. *Soc Interface*. 2015;12:20150066.
77. Nguyen TD. A Comparison of a nonlinear and quasilinear viscoelastic anisotropic model for fibrous tissues. In: Garikipati

K, Arruda EM, eds. *IUTAM Symposium on Cellular, Molecular and Tissue Mechanics*. The Netherlands: Springer Netherlands; 2010:19–29.

78. Chung CW, Buist ML. A novel nonlinear viscoelastic solid model. *Nonlinear Anal Real World Appl*. 2012;13:1480–1488.
79. Sigal IA, Grimm JL, Schuman JS, Kagemann L, Ishikawa H, Wollstein G. A method to estimate biomechanics and mechanical properties of optic nerve head tissues from parameters measurable using optical coherence tomography. *IEEE Trans Med Imaging*. 2014;33:1381–1389.
80. Sigal IA. An applet to estimate the IOP-induced stress and strain within the optic nerve head. *Invest Ophthalmol Vis Sci*. 2011;52:5497–5506.
81. Bellezza AJ, Hart RT, Burgoyne CF. The optic nerve head as a biomechanical structure: initial finite element modeling. *Invest Ophthalmol Vis Sci*. 2000;41:2991–3000.
82. Asejczyk-Widlicka M, Śródka DW, Kasprzak H, Iskander DR. Influence of intraocular pressure on geometrical properties of a linear model of the eyeball: effect of optical self-adjustment. *Optik - International Journal for Light and Electron Optics*. 2004;115:517–524.
83. Sigal IA, Flanagan JG, Tertinegg I, Ethier CR. Modeling individual-specific human optic nerve head biomechanics. Part I: IOP-induced deformations and influence of geometry. *Biomech Model Mechanobiol*. 2009;8:85–98.
84. Sigal IA, Flanagan JG, Tertinegg I, Ethier CR. Modeling individual-specific human optic nerve head biomechanics. Part II: influence of material properties. *Biomech Model Mechanobiol*. 2009;8:99–109.
85. Coudrillier B, Pijanka JK, Jefferys JL, et al. Glaucoma-related changes in the mechanical properties and collagen microarchitecture of the human sclera. *PLoS One*. 2015;10:e0131396.
86. Roberts MD, Liang Y, Sigal IA, et al. Correlation between local stress and strain and lamina cribrosa connective tissue volume fraction in normal monkey eyes. *Invest Ophthalmol Vis Sci*. 2010;51:295–307.

Investigative Ophthalmology & Visual Science